Impact of pressure on plastic yield in amorphous solids with open structure

B. Mantisi

*Laboratoire de Physique Théorique de la Matière Condensée, Paris Sorbonne Universités UPMC, BP 121, 4 Place Jussieu,
75252 Paris Cedex 05, France*

G. Kermouche

*Materials Sciences and Structures Division, Ecole des Mines de Saint-Etienne, LGF UMR No. 5307, CNRS, 158 Cours Fauriel,
42023 Saint-Etienne Cedex 2, France*

E. Barthel

*École Supérieure de Physique et de Chimie Industrielles de la Ville de Paris ParisTech, PSL Research University,
Sciences et Ingénierie de la matière Molle, CNRS UMR No. 7615, 10 Rue Vauquelin, F-75231 Paris Cedex 05, France
and Sorbonne-Universités, UPMC Université Paris 06, SIMM, 10 Rue Vauquelin, 75231 Paris Cedex 05, France*

A. Tanguy

Université de Lyon, LaMCoS, INSA-Lyon, CNRS UMR5259, F-69621, France

Plasticity in amorphous silica is unusual: The yield stress decreases with hydrostatic pressure, in contrast to the Mohr-Coulomb response commonly found in more compact materials such as bulk metallic glasses. To better understand this response, we have carried out molecular dynamics simulations of plastic response in a model glass with open structure. The simulations reproduce the anomalous dependence of yield stress with pressure and also correctly predict that the plastic response turns to normal once the material has been fully compacted. We also show that the overall shape of the yield surface is consistent with a quadratic behavior predicted assuming local buckling of the structure, a point of view that fits well into the present understanding of the deformation mechanisms of amorphous silica. The results also confirm that free volume is an adequate internal variable for a continuum scale description of the plastic response of amorphous silica. Finally, we also investigate the long-range correlations between rearrangement events. We find that strong intermittency is observed when the structure remains open, while compaction results in more homogeneous rearrangements. These findings are in agreement with recent results on the effect of compression on the middle range order in silicate glasses and also suggest that the well-known volume recovery of densified silica at relatively low temperatures is in fact a form of aging.

I. INTRODUCTION

One of the main challenges in the field of amorphous materials is to establish relations between atomic scale processes and continuum scale descriptions of mechanical behavior (constitutive laws). For bulk metallic glasses a relatively consistent picture has emerged. It has been evidenced both experimentally [1] and numerically [2] that the yield stress increases with application of hydrostatic pressure. The idea that local rearrangements are hampered by compressive stress acting normal to the shear direction ties in with the accepted effect of pressure in the jamming transition [3]. As a result, Mohr-Coulomb law or similar constitutive laws with moderate yield-pressure coupling constants are usually found adequate [4,5]. In these constitutive laws, Spaepen's free volume [6] is often used as the state variable. At the same time, limitations in the free volume view of the deformation of bulk metallic glasses have arisen, especially related to local instabilities and the formation of shear bands. Other pictures have been proposed, involving more structural information, such as shear transformation zones [7–9] or a liquidlike environment [10]. Implications for constitutive equations are not completely clear and to date there is still no comprehensive understanding of the plasticity of amorphous solids across length scales [11,12].

To better identify generic mechanisms of plastic deformation in amorphous solids, it is interesting to consider other glassy materials with a widely different plastic response. Because of its very large free volume retained from a covalent liquid state, amorphous silica compacts under pure hydrostatic pressure above a threshold of approximately 10 GPa, resulting in irreversible volumetric strain, i.e., densification [13]. An additional observation is that shear lowers the densification threshold [14]. Recently, there have been attempts to derive constitutive equations to account for this unconventional plastic response [15–17], but the respective roles of densification and shear flow remain controversial [18]. To better understand the plastic behavior of amorphous materials with an open structure and its implications in terms of plastic rearrangement mechanisms, we have carried out a numerical investigation of yield in a model system emulating amorphous silica. In a previous work [19] we investigated densification under pure hydrostatic pressure and yield under pure shear at constant volume. However, to analyze plastic response from a continuum mechanics point of view, we need to consider mixed pressure-shear types of loading, which is the aim of the present paper. Our results evidence a reduction of shear yield stress with pressure at lower pressures, while plasticity becomes normal after full compaction. This evolution

033001-1

qualitatively reproduces experimental facts and can be compared to previously proposed constitutive models. We also show that the shape of the resulting yield surface is parabolic, as suggested by a simple buckling model initially proposed by Lambropoulos *et al.* [15]. This observation ties in with the established specific deformation mechanism of the open structure at lower pressures. Finally, we evidence that, beyond this local picture of deformation, compaction results in a more homogeneous deformation process, an observation that we link to known structural effects of pressure on silicate glasses.

II. METHOD

Molecular dynamics was used to build a numerical model emulating silica glass, with a truncated and smoothed van Beest–Kramer–van Santen potential [20–22]. This potential has been shown to provide an accurate relation between density and pressure and more generally to adequately simulate most of the specificities of silica samples [23]. Following our previous protocol [19], we prepared the sample from an initial stable crystal state (β cristobalite), increased the temperature to 5200 K (twice the melting temperature), and let the system evolve over 1 ns to ensure diffusion. The temperature was imposed through a Nosé-Hoover thermostat with a temperature damping parameter $\delta t = 10^{-15}$ s. Then we quenched the sample to reach 10^{-5} K at a quenching rate of 5.2×10^{12} K s^{-1}. This quench rate has been chosen based on detailed studies in the literature [24–26]. It provides an adequate initial structure of the glass for samples relaxed to 0 ± 0.001 GPa. The structure was validated through comparisons of density, pair distribution function, static structure factor, and angle distribution with experimental results on amorphous silica [19]. To ensure that our results are not affected by finite-size effects, we built samples with $N = 24.000$ (size 7.6 nm) and $N = 81.000$ particles (size 10.2 nm), for which no significant difference was observed. During evolution, the strain increments were 1×10^{-4}. Significantly larger increments result in increasing plastic events due to the rate effect.

III. MACROSCOPIC PLASTIC RESPONSE OF A MODEL MATERIAL WITH OPEN STRUCTURE

The samples were loaded hydrostatically at various pressures ranging from 0 to 20 GPa and annealed [19]. For each of these pressures, we carried out quasistatic shear loading-unloading runs at constant hydrostatic pressure. We explored a wide range of maximum shear strain, from 0 to 25% strain.

A few representative curves for shear loading and unloading are plotted for different hydrostatic pressures in Fig. 1. Shear was quantified from the difference between principal stress values. We find a two-stage behavior as hydrostatic pressure increases. For pressures lower than 8 GPa [Fig. 1(a)], the yield threshold decreases significantly with pressure. Above 8 GPa the yield threshold increases again, but more slowly, in a manner consistent with Mohr-Coulomb law. The plastic flow stress, measured at large strains (25%), is almost unaffected by pressure, so at low pressures a yield peak is observed, followed by softening. Around 5 GPa the peak vanishes to be replaced by moderate hardening.
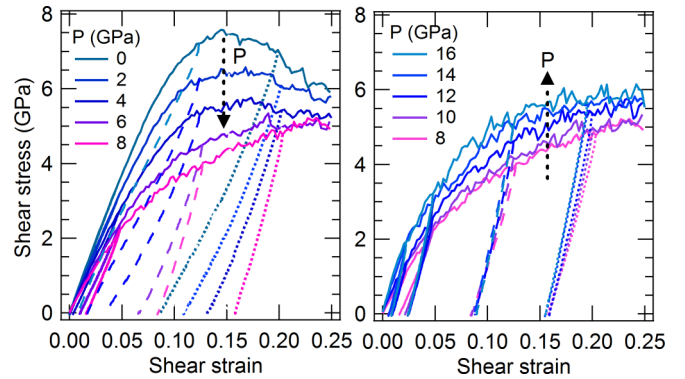

FIG. 1. Shear stress vs shear strain calculated for an amorphous material with open structure for different hydrostatic pressures (on the left from 0 to 8 GPa and the right from 8 to 16 GPa). The dashed and dotted lines are unloads after partial loading at various strains. At low pressures, the yield stress in shear decreases with pressure, with a yield peak and softening. Around 5 GPa the peak vanishes. Above 8 GPa the trend is reversed and the yield stress increases with pressure.

This evolution of the stress-strain relation in shear is consistent with our previous results at constant volume. In particular, predensification of the amorphous material (by application of elevated pressures and unloading before shear) was found to suppress the yield peak [19], in a manner somewhat analogous to the effect of high pressure during shear described here.

From these loading-unloading runs, we quantified the plastic strain of our model material as a function of loading, for a large set of maximum hydrostatic pressures and maximum shear stresses. Both densification and residual shear strain were calculated by unloading to zero shear stress and zero hydrostatic pressure. The results are plotted as isoshear-isostrain and isodensity lines in a von Mises stress vs hydrostatic pressure map (Fig. 2), delineating a yield surface. At zero pressure, yield in shear occurs around 12.5 GPa, but this threshold is found to decrease significantly with hydrostatic pressure. Still, below a hydrostatic pressure of about 5 GPa, plastic yielding is dominated by shear: Isoshear lines slope down roughly linearly. They are closely spaced due to the onset of softening following the yield peak and densification is very moderate. When pressure exceeds 5 GPa, the isoshear lines increasingly spread out, indicative of the transition to a hardening behavior. Simultaneously, the isodensity lines become denser, signaling the onset of densification. In this region, isoshear and isodensity lines also gradually diverge: The isoshear lines level off and even start to increase slowly with pressure above 10 GPa, while the isodensity lines slope down more and more precipitously to meet the pressure axis with a sharp angle.

Through all these features the calculated plastic response emulates the known behavior of amorphous silica fairly well. As in silica, significant densification is observed and it is facilitated by shear [14]. We also observe that silica can simultaneously undergo densification *and* conventional plastic shear flow, a deformation mode for which there is also experimental evidence both old [13] and more recent [27,28].
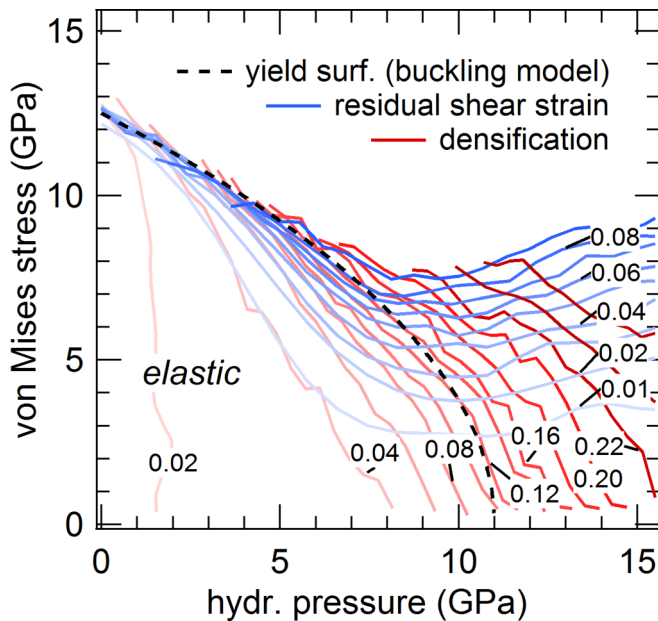
FIG. 2. Distribution of residual volumetric strain (densification) and residual shear strain as a function of loading (maximum hydrostatic pressure and maximum von Mises stress). This map delineates a yield surface with strain hardening. A simple buckling instability model (1) predicts the overall parabolic shape of the surface quite accurately.

Finally, our results demonstrate that just as shear facilitates densification, hydrostatic pressure lowers the shear yield threshold. Indeed, early diamond anvil cell experiments have shown that for amorphous silica, the shear yield threshold initially decreases with pressure to increase again above about 10 GPa [29]. In summary, the present results validate our calculation parameters for a qualitative description of the plastic deformation of open structure materials such as amorphous silica.

IV. LOCAL STRUCTURAL REARRANGEMENTS AND BUCKLING PICTURE

We now turn to the local rearrangement process at work during compression. Defining the free volume as the fraction of voids per unit material volume, with reference to the more compact crystalline forms, it is found that in pristine amorphous silica the free volume is considerable, reaching about 20%. It has long been known that compaction primarily results from a reduction of this free volume while leaving interatomic distances constant. A very direct demonstration of this peculiar deformation process has been brought fairly recently by positron annihilation [30]. The same process is also clearly evidenced in diffraction experiments: In the structure factor, the free volume is manifest as an additional peak at smaller wave vectors, the so-called first sharp diffraction peak (FSDP), which comes in addition to the usual correlation peaks reflecting interatomic distances. Experimentally, when pressure is applied, the intensity of the FSDP decreases sharply and the peak shifts markedly towards the larger wave vectors [31]. Here this experimental evolution is perfectly
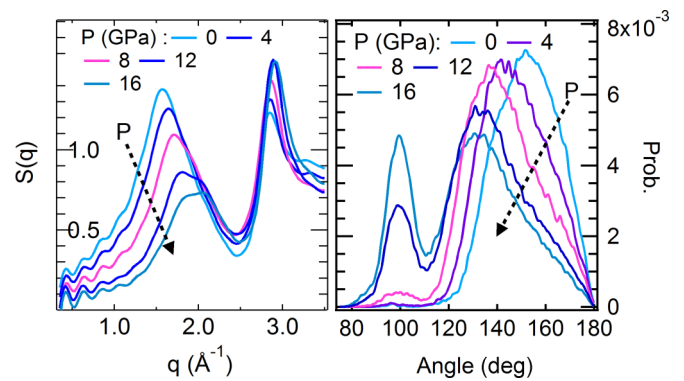

FIG. 3. Shown on the left is the structure factor calculated under pressure at zero shear. The reduction of the free volume predominantly affects the first sharp diffraction peak around 1.5 Å^{-1}, which reflects the collapse of the open structure. The signature of the short-range order at higher wave vectors is much less affected. Shown on the right is the Si-O-Si angle distribution as a function of pressure. Hydrostatic compression shifts the distribution to lower angles.

reproduced: In the calculated structure factor (Fig. 3, left), the FSDP decreases and shifts as expected while the diffraction peaks at higher wave vectors stay nearly unaffected, an evolution that signals the collapse of the open structure at intermediate length scales while interatomic distances remain constant.

The kinematics of this compaction at constant interatomic bond length is mediated by intertetrahedral rotations and bending, as most clearly demonstrated experimentally by the comparison of partial structure factors in GeO_2 [32], a glass analogous to amorphous silica. Further more immediate evidence of the evolution of bond angle distribution during compression is found in Raman spectroscopy: With compaction, the Raman main band around 440 cm^{-1} shifts to higher wave numbers and becomes narrower, reflecting a decrease of both average bond angle and distribution width [33,34]. For our open structure model, the distribution of intertetrahedral bond angles has been calculated as a function of pressure and is displayed in Fig. 3 (right), exhibiting a strong shift of the distribution towards lower angles as expected.

There is a large body of evidence to demonstrate that in amorphous silica, the specific deformation mechanisms of the open structure, connected to the evolutions of the FSDP and bond angle distribution just detailed, correlate with a strikingly anomalous thermomechanical behavior including a low thermal expansion coefficient and increasing elastic moduli with temperature [35], excess sound absorption at low temperature [36], and a low Poisson ratio [37], which increases with stretch [38]. The archetypal anomaly, however, is found in the compressibility that increases with pressure. This surprising trend was evidenced by Bridgman [39], who readily ascribed it to the open structure of silica. Conversely, an increase of the tensile modulus with increasing tension is observed [38]. This nonlinearity gradually disappears for glasses with less open structures (Mallinder's filled glasses) [38,39] or when silica is densified [40,41].

This elastic nonlinearity has qualitatively been reproduced by molecular dynamics simulations [42,43]. Here we observe

a similar nonlinearity at low pressures, as also previously [19]. This nonlinearity, which is apparent in the loading but also in the partial unloading curves (Fig. 1, dotted and dashed lines), gradually disappears above 8 GPa.

Huang and Kieffer have proposed an insightful analogy for the reduction of the stiffness of amorphous silica under pressure. In the transition from β to α cristobalite, the higher density phase exhibits the lower elastic moduli [42]. Of course, in the amorphous structure, we are confronted with a large distribution of configurations, so why does the comparison hold? Early qualitative explanations for the thermomechanical anomalies focused on the bending of the Si-O-Si bond and the ensuing softening of the local structure [38,44,45] when this angle decreases under compression. Similarly, in the α-β transition of cristobalite, the more open structure enjoys higher rigidity while the similarly connected but more folded structure is mechanically more compliant.

This idea of some structural bending or folding coupled to softening is in fact strongly reminiscent of the mechanical concept of buckling. Following this line of thought, Lambropoulos *et al.* suggested that local buckling of the open structure of silica should account for the pressure dependence of the yield threshold [15]. They performed a simple finite-element calculation of the buckling instability of a simple beam array. Their results suggest that the instability threshold τ can be expressed as

$$\frac{\tau}{\tau_c} = \sqrt{1 - \frac{p}{p_c}}, \qquad (1)$$

where p is the pressure, p_c the buckling pressure (without shear), and τ_c a critical shear at vanishing pressure. This parabolic shape is the dashed line plotted in Fig. 2, which satisfactorily describes the yield surface determined from the much more involved molecular dynamics simulations. There are two adjustable parameters $\tau_c = 12.5$ GPa and $p_c = 11.0$ GPa. Interestingly, this yield surface curves down to zero near a compression threshold of approximately 10 GPa, in close analogy to a criterion we proposed recently [16] to model the density distribution after indentation in amorphous silica. These yield surfaces differ, however, in the vicinity of pure shear loading, with a yield threshold (12.5 GPa) that exceeds the 7.5 GPa also derived from silica pillar compression experiments [27].

In summary, given the propensity of open amorphous structures to compact through intertetrahedral bending and rotation, it has been argued that the ensuing mechanical softening results from buckling [15]. Indeed, we find that a simple buckling model qualitatively accounts for the shape of the yield surface we have found in our numerical calculations. Moreover, we note that the concept of buckling in fact underpins at least several of the standard explanations of the thermomechanical anomalies of silica such as reduced thermal expansion [44] and inverse nonlinear elasticity [38,42,46].

The strong coupling between the plastic yield and free volume (yield depends on free volume, which in turn is affected by yield) apparently invalidates the notion of a well defined amorphous material with approximately 20% free volume. Indeed, our results provide both physical motivation and qualitative inputs for refined continuum scale descriptions

of the constitutive behavior of amorphous silica, with the decreasing free volume playing the role of an internal variable, as already implemented in some earlier constitutive relations for amorphous silica [16].

V. PLASTIC REARRANGEMENTS AND MIDDLE RANGE ORDER

The previous section was devoted to a local picture of rearrangements in connection with bulk mechanical response. In the field of amorphous materials, however, the correlation between rearrangements and the heterogeneity of their distribution are central questions, which can be explored in molecular dynamics simulations as well. For that purpose, we have quantified the nonaffine displacement field [19], which is the difference between the real calculated atomic displacements and the homogeneous affine displacements at the same position. To illustrate the impact of pressure, maps of typical nonaffine displacement fields taken at 7.5% shear strain are shown in Fig. 4 for hydrostatic pressures equal to 0, 5, and 10 GPa. At 0 GPa, Fig. 4(a) displays a typical isolated event with large magnitude, affecting a sizable fraction of the simulation cell. At 5 GPa, the typical snapshot [Fig. 4(b)] exhibits a few individualized events with smaller spatial extent. At 10 GPa [Fig. 4(c)] the cell is filled with a continuous flow of even smaller sized events. Qualitatively, we find a strong effect of pressure on the long-range kinematics of plastic deformation, with rearrangements becoming smaller but more numerous as pressure increases. More quantitatively, we have also calculated the participation ratio [19] at each shear step. It is a measure of the fraction of atoms that move together during one displacement step and goes from $1/N$ for the isolated motion of a single atom to 1 for a block motion of the full system. The participation ratio is plotted as a function of shear strain for different hydrostatic pressures in Fig. 5 (left). For low pressures, series of events with very large participation ratios are evidenced: The participation ratio abruptly switches between very large values, close to 1/2 (involving about half of the cell atoms), and values of the order of 1/100, involving groups of a few hundred atoms. This strong intermittency disappears as hydrostatic pressure increases: The large-scale events are gradually suppressed and vanish above 5 GPa. For a more quantitative assessment, we use increment statistics as developed for the analysis of turbulence [47]. As a measure of intermittency, we calculate the distribution of the jumps of participation ratio for each strain increment (Fig. 5 right) and evaluate the impact of pressure. We find that for all the pressures investigated here, the low-amplitude jumps (roughly less than 0.03) follow an exponential distribution and the characteristic jump size decreases with pressure to saturate around 15 GPa (Fig. 5, right, inset). Moreover, at low pressures, a tail adds up to this exponential component, accounting for scarce events with large amplitudes. Increasing pressure drastically reduces this tail contribution, gradually suppressing all events with large participation ratios. In brief, we find that when the structure collapses under pressure, large-scale rearrangements are suppressed and the fluctuations of the small-scale events are also reduced. These results show that under pressure the local rearrangement processes are more homogeneous, an evolution that also parallels the impact of
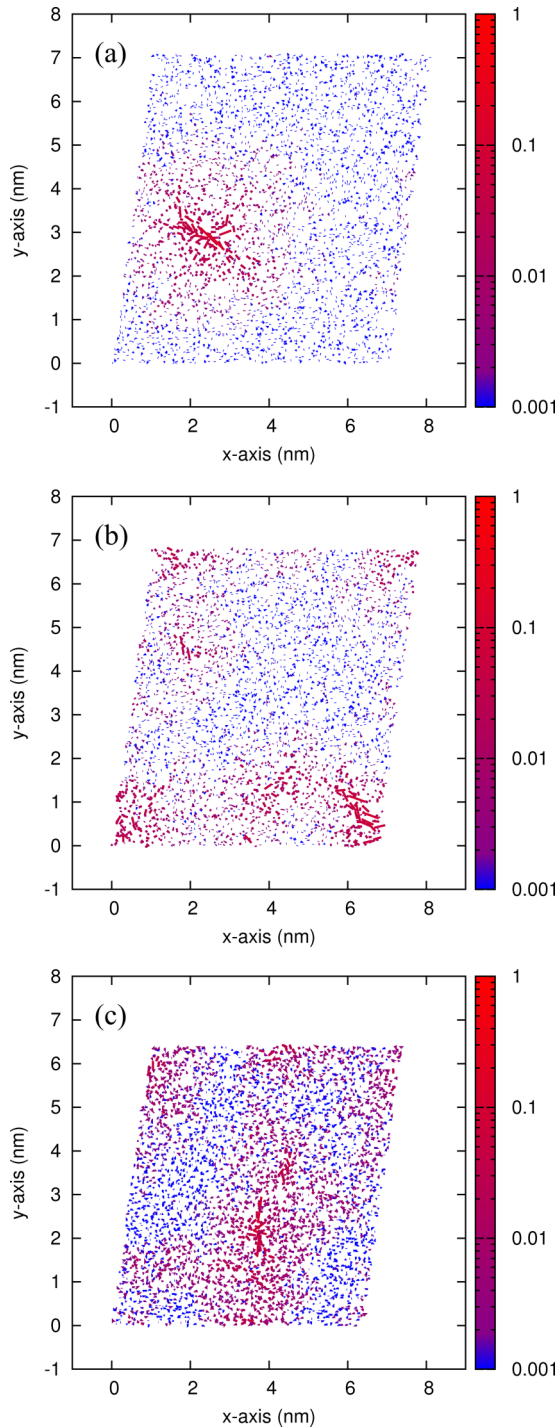
FIG. 4. Nonaffine displacement maps (representative cross sections, amplitudes in Å) taken at 7.5% shear strain for hydrostatic pressures equal to (a) 0 GPa, (b) 5 GPa, and (c) 10 GPa.
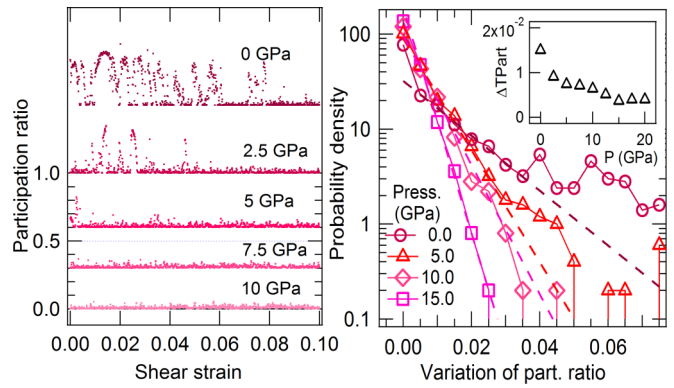

FIG. 5. Shown on the left is the participation ratio for rearrangements as a function of shear strain, for increasing hydrostatic pressures (the plots have been offset for clarity). Shown on the right is the probability density of the jumps of participation ratio as a function of jump amplitude, during loading. The large-amplitude events are gradually suppressed by increasing the hydrostatic pressure, while the fluctuations of the characteristic size decrease.

predensification we observed in our earlier simulations of shear at constant volume [19].

No experimental technique is presently capable of monitoring the spatiotemporal correlation between plastic events in amorphous silicates under strain. However, progress has recently been registered in the study of middle range order in silicate glasses with open structure such as amorphous silica. In particular, an impact of compaction on middle

range order in the amorphous structure has been observed. Homogeneity of the structure at length scales of the order of 1 nm can be probed by small-angle x-ray scattering (SAXS). In borosilicate glasses, which also feature an open structure, a reduction of the structure factor in the small wave vector region (below the FSDP) was found when the glasses were prepared under pressure [48]. For silica itself, due to the very high glass transition temperature, it is difficult to obtain large and homogeneously densified samples adequate for SAXS and similar data are lacking. However, related evidence in the dynamic response of amorphous silica has been obtained from the Brillouin scattering of x-ray radiations. It was found that at these wavelengths, the damping of acoustic modes exhibits two very different regimes, with a crossover that reflects the typical size of the elastic heterogeneities [49]. This size, which was found to be about 6 nm in pristine silica, shrinks to 3 nm for densified silica, pointing again to an effective homogenization of the material with densification [50,51]. Directly connected to this reduction of the intermediate range disorder with pressure, the boson peak in silica and other open structure glasses is found to shift to higher frequencies when density increases, in both the reversible [34] and the irreversible deformation regimes [31,52,53]. Simultaneously, the amplitude decreases.

In brief, the more expanded state exhibits more structural heterogeneity and more intermittent rearrangement processes. At this point it is interesting to point out that densified silica relaxes amazingly easily. Indeed, despite a glass transition temperature of the order of 1500° C, significant free volume recovery is observed at temperatures as low as 200° C [54] and small but measurable recovery has even been observed at room temperature provided the material is allowed to evolve over a period of 5 yr [55]. Therefore, free volume recovery in densified silica may be seen as an aging process during which structural heterogeneities develop and the yield threshold increases, finally leading, as in the present simulations, to intermittency [56,57]. Conversely, compaction is a form of rejuvenation.

VI. CONCLUSION

Through molecular dynamics simulations, we have studied the impact of hydrostatic pressure on the plastic response of an amorphous material with open structure. This material qualitatively emulates amorphous silica. Through the investigation of the response under combined loading in pressure and shear, we have obtained a detailed description of yield. There is densification during plastic yielding and the yield threshold in shear decreases with pressure. Above a definite threshold, hardening is found. In keeping with prior understanding of the anomalous thermomechanical properties of silica, we have shown that the shape of the yield surface is consistent with a model involving local buckling of the open structure of the material. We also found that the free volume seems to be a very relevant internal variable for constitutive relations of amorphous silica. In addition, we have directly demonstrated the impact of free volume on the long-range correlation

between rearrangement processes: While intermittency is present during yielding of the open structure, compaction suppresses large-scale rearrangements and decreases the size of the local fluctuations. This observation is consistent with the recently demonstrated evolution of amorphous silica towards a more homogeneous structure at the middle range upon compaction. From this same point of view, the well known volume recovery of densified silica at low temperatures can be seen as an aging process.

[1] C. A. Schuh, T. C. Hufnagel, and U. Ramamurty, Acta Mater. **55**, 4067 (2007).
[2] C. A. Schuh and A. C. Lund, Nat. Mater. **2**, 449 (2003).
[3] A. J. Liu and S. R. Nagel, Nature (London) **396**, 21 (1998).
[4] L. Anand and C. Su, J. Mech. Phys. Solids **53**, 1362 (2005).
[5] Y. Gao, Model. Simul. Mater. Sci. Eng. **14**, 1329 (2006).
[6] F. Spaepen, Acta Metall. **25**, 407 (1977).
[7] A. Argon, Acta Metall. **27**, 47 (1979).
[8] A. Argon and L. T. Shi, Acta Metall. **31**, 499 (1983).
[9] M. L. Falk and J. S. Langer, Annu. Rev. Condens. Matter Phys. **2**, 353 (2011).
[10] M. J. Demkowicz and A. S. Argon, Phys. Rev. B **72**, 245205 (2005).
[11] M. Falk and C. Maloney, Eur. Phys. J. B **75**, 405 (2010).
[12] D. Rodney, A. Tanguy, and D. Vandembroucq, Model. Simul. Mater. Sci. Eng. **19**, 083001 (2011).
[13] D. M. Marsh, Proc. R. Soc. London Ser. A **279**, 420 (1964).
[14] J. Mackenzie, J. Am. Ceram. Soc. **46**, 461 (1963).
[15] J. C. Lambropoulos, S. Xu, and T. Fang, J. Am. Ceram. Soc. **79**, 1441 (1996).
[16] G. Kermouche, E. Barthel, D. Vandembroucq, and P. Dubujet, Acta Mater. **56**, 3222 (2008).
[17] V. Keryvin, J.-X. Meng, S. Gicquel, J.-P. Guin, L. Charleux, J.-C. Sangleboeuf, P. Pilvin, T. Rouxel, and G. Le Quilliec, Acta Mater. **62**, 250 (2014).
[18] V. Keryvin, S. Gicquel, L. Charleux, J. P. Guin, M. Nivard, and J. C. Sangleboeuf, Key Eng. Mater. **606**, 53 (2014).
[19] B. Mantisi, A. Tanguy, G. Kermouche, and E. Barthel, Eur. Phys. J. B **85**, 304 (2012).
[20] B. W. H. van Beest, G. J. Kramer, and R. A. van Santen, Phys. Rev. Lett. **64**, 1955 (1990).
[21] A. Carré, L. Berthier, J. Horbach, S. Ispas, and W. Kob, J. Chem. Phys. **127**, 114512 (2007).
[22] F. Yuan and L. Huang, Sci. Rep. **4**, 5035 (2014).
[23] B. Cowen and M. El-Genk, Comput. Mater. Sci. **107**, 88 (2015).
[24] J. A. N. Zasadzinski, J. Microsc. **150**, 137 (1988).
[25] K. Vollmayr, W. Kob, and K. Binder, Phys. Rev. B **54**, 15808 (1996).

[26] R. Vuilleumier, N. Sator, and B. Guillot, Geochim. Cosmochim. Acta **73**, 6313 (2009).
[27] R. Lacroix, G. Kermouche, J. Teisseire, and E. Barthel, Acta Mater. **60**, 5555 (2012).
[28] D. Wakabayashi, N. Funamori, and T. Sato, Phys. Rev. B **91**, 014106 (2015).
[29] C. Meade and R. Jeanloz, Science **241**, 1072 (1988).
[30] M. Zanatta, G. Baldi, R. S. Brusa, W. Egger, A. Fontana, E. Gilioli, S. Mariazzi, G. Monaco, L. Ravelli, and F. Sacchetti, Phys. Rev. Lett. **112**, 045501 (2014).
[31] S. Sugai and A. Onodera, Phys. Rev. Lett. **77**, 4210 (1996).
[32] S. Sampath, C. J. Benmore, K. M. Lantzky, J. Neuefeind, K. Leinenweber, D. L. Price, and J. L. Yarger, Phys. Rev. Lett. **90**, 115502 (2003).
[33] R. J. Hemley, H. K. Mao, P. M. Bell, and B. O. Mysen, Phys. Rev. Lett. **57**, 747 (1986).
[34] T. Deschamps, C. Martinet, D. Neuville, D. de Ligny, C. Coussa-Simon, and B. Champagnon, J. Non-Cryst. Solids **355**, 2422 (2009).
[35] R. Brückner, J. Non-Cryst. Solids **5**, 123 (1970).
[36] B. E. White, Jr. and R. O. Pohl, Phys. Rev. Lett. **75**, 4437 (1995).
[37] T. Rouxel, H. Ji, T. Hammouda, and A. Moreac, Phys. Rev. Lett. **100**, 225501 (2008).
[38] F. Mallinder and B. Proctor, Phys. Chem. Glasses **5**, 91 (1964).
[39] P. Bridgman, Am. J. Sci. **58**, 359 (1925).
[40] C.-s. Zha, R. J. Hemley, H.-k. Mao, T. S. Duffy, and C. Meade, Phys. Rev. B **50**, 13105 (1994).
[41] T. Rouxel, H. Ji, J. Guin, F. Augereau, and B. Rufflé, J. Appl. Phys. **107**, 094903 (2010).
[42] L. Huang and J. Kieffer, Phys. Rev. B **69**, 224203 (2004).
[43] Y. Liang, C. R. Miranda, and S. Scandolo, Phys. Rev. B **75**, 024205 (2007).
[44] H. T. Smyth, J. Am. Ceram. Soc. **38**, 140 (1955).
[45] F. M. Ernsberger, in *Elasticity and Strength in Glasses: Glass: Science and Technology*, edited by D. Uhlmann and N. J. Kreidl (Academic, New York, 1980), Vol. 5, pp. 1–18.
[46] M. Vukcevich, J. Non-Cryst. Solids **11**, 25 (1972).

[47] E. Falcon, S. Fauve, and C. Laroche, Phys. Rev. Lett. **98**, 154501 (2007).

[48] S. Reibstein, L. Wondraczek, D. De Ligny, S. Krolikowski, S. Sirotkin, J.-P. Simon, V. Martinez, and B. Champagnon, J. Chem. Phys. **134**, 204502 (2011).

[49] B. Rufflé, M. Foret, E. Courtens, R. Vacher, and G. Monaco, Phys. Rev. Lett. **90**, 095502 (2003).

[50] G. Baldi, V. Giordano, G. Monaco, and B. Ruta, J. Non-Cryst. Solids **357**, 538 (2011).

[51] G. Baldi, M. Zanatta, E. Gilioli, V. Milman, K. Refson, B. Wehinger, B. Winkler, A. Fontana, and G. Monaco, Phys. Rev. Lett. **110**, 185503 (2013).

[52] B. Mantisi, S. Adichtchev, S. Sirotkin, L. Rafaelly, L. Wondraczek, H. Behrens, C. Marcenat, N. Surovtsev, A. Pillonnet, E. Duval, B. Champagnon, and A. Mermet, J. Phys. Condens. Matter **22**, 025402 (2010).

[53] S. Fuhrmann, T. Deschamps, B. Champagnon, and L. Wondraczek, J. Chem. Phys. **140**, 054501 (2014).

[54] J. Mackenzie, J. Am. Ceram. Soc. **46**, 470 (1963).

[55] A. Polian and M. Grimsditch, Phys. Rev. B **41**, 6086 (1990).

[56] P. Yunker, Z. Zhang, K. B. Aptowicz, and A. G. Yodh, Phys. Rev. Lett. **103**, 115701 (2009).

[57] T. Kajiya, T. Narita, V. Schmitt, F. Lequeux, and L. Talini, Soft Matter **9**, 11129 (2013).